

A Linear-Programming Approximation of AC Power Flows

Carleton Coffrin, *Member, IEEE*, Pascal Van Hentenryck, *Member, IEEE*

Abstract—Linear active-power-only DC power flow approximations are pervasive in the planning and control of power systems. However, these approximations fail to capture reactive power and voltage magnitudes, both of which are necessary in many applications to ensure voltage stability and AC power flow feasibility. This paper proposes linear-programming models (the LPAC models) that incorporate reactive power and voltage magnitudes in a linear power flow approximation. The LPAC models are built on a convex approximation of the cosine terms in the AC equations, as well as Taylor approximations of the remaining nonlinear terms. Experimental comparisons with AC solutions on a variety of standard IEEE and MATPOWER benchmarks show that the LPAC models produce accurate values for active and reactive power, phase angles, and voltage magnitudes. The potential benefits of the LPAC models are illustrated on two “proof-of-concept” studies in power restoration and capacitor placement.

Index Terms—DC power flow, AC power flow, LP power flow, linear relaxation, power system analysis, capacitor placement, power system restoration

NOMENCLATURE

\tilde{I}	AC Current
$\tilde{V} = v + i\theta$	AC voltage
$\tilde{S} = p + iq$	AC power
$\tilde{Z} = r + ix$	Line impedance
$\tilde{Y} = g + ib$	Line admittance
$\tilde{Y}^b = g^y + ib^y$	Y-Bus element
$\tilde{Y}^c = g^c + ib^c$	Line charge
$\tilde{Y}^s = g^s + ib^s$	Bus shunt
$\tilde{T} = t + is$	Transformer parameters
$\tilde{V} = \tilde{V} \angle\theta^\circ$	Polar form
\tilde{S}_n	AC Power at bus n
\tilde{S}_{nm}	AC Power on a line from n to m
\mathcal{PN}	Power network
N	Set of buses in a power network
L	Set of lines in a power network
G	Set of voltage controlled buses
s	Slack Bus
$ \tilde{V}^h $	Hot-Start voltage magnitude
$ \tilde{V}^t $	Target voltage magnitude
ϕ	Voltage magnitude change
Δ	Absolute difference
δ	Percent difference
\hat{x}	Approximation of x
\bar{x}	Upper bound of x
\underline{x}	Lower bound of x

I. INTRODUCTION

OPTIMIZATION technology is widely used in modern power systems [1] and has resulted in millions of dollars in savings annually [2]. But the increasing role of demand response, the integration of renewable sources of energy, and the desire for more automation in fault detection and recovery pose new challenges for the planning and control of electrical power systems [3]. Power grids now need to operate in more stochastic environments and under varying operating conditions, while still ensuring system reliability and security.

Optimization of power systems encompasses a broad spectrum of problem domains, including optimal power flow [4], [5], [6], [7], [8], [9], [10], [11], [12], [13], [14], LMP-base market calculations [15], [16], [17], transmission switching [18], [19], [20], real-time security-constrained dispatch [21], [22], day-ahead security-constrained unit commitment [23], [24], [25], distribution network configuration [26], [27], capacitor placement [28], [29], [30], expansion planning [31], [32], [33], [34], [35], [36], [37], [38], [39], vulnerability analysis [40], [41], [42], [43], [44], and power system restoration [45], [46] to name a few. Some of these use active power only, while others consider both active and reactive power.

Restricting attention to active power is often appealing computationally as the nonlinear AC power flow equations can then be approximated by a set of linear equations that define the so-called Linearized DC (LDC) model. Under normal operating conditions and with some adjustment for line losses, the LDC model produces a reasonably accurate approximation of the AC power flow equations for active power [47]. Moreover, the LDC model can be embedded in Mixed-Integer Programming (MIP) models for a variety of optimization applications in power system operations. This is particularly attractive as the computational efficiency of Linear Programming (LP) and MIP solvers has significantly improved over the last two decades [48].

However, the LDC model does not capture reactive power and hence cannot be used for applications such as capacitor placement and voltage stability to name only two. Moreover, the accuracy of the LDC model outside normal operating conditions is an open point of discussion (e.g., [15], [47], [49], [50], [51]). This in turn raises concerns for other applications such transmission planning, vulnerability analysis, and power restoration, which may return infeasible or suboptimal solutions when the LDC model is used to approximate the AC power flow equations. As a result, these applications often turn to nonlinear programming techniques [8], [13], [14], [17], iterative heuristics and decomposition [11], [12], [36],

[42], model relaxation [7], [28], tabu search [30], and genetic algorithms [29], [34] to ensure feasibility. These techniques often require extensive tuning for each problem domain, may consume significant computational resources, and cannot guarantee global optimality.

This paper aims at bridging the gap between the LDC model and the AC power flow equations. It presents linear programs to approximate the AC power flow equations. These linear programs, called the LPAC models, are based on two ideas:

- 1) They reason both on the voltage phase angles and the voltage magnitudes, which are coupled through equations for active and reactive power;
- 2) They use a piecewise linear approximation of the cosine term in the power flow equations and Taylor series for approximating the remaining nonlinear terms.

The LPAC models have been evaluated experimentally over a number of standard benchmarks under normal operating conditions and various contingencies. Experimental comparisons with AC solutions on standard IEEE and MatPower benchmarks shows that the LPAC models are highly accurate for active and reactive power, phase angles, and voltage magnitudes. Moreover, the LPAC models can be integrated in MIP models for applications reasoning about reactive power (e.g., capacitor placement) or topological changes (e.g., transmission planning, vulnerability analysis, and power restoration).

This rest of this paper presents a rigorous and systematic derivation of the LPAC models, experimental results about their accuracy, and its application to power restoration and capacitor placement. Section II reviews the AC power flow equations. Section III derives the LPAC models and Section IV presents the experimental results on its accuracy. Section V presents the “proof-of-concept” experiments in power restoration and capacitor placement to demonstrate potential applications of the LPAC models. Section VI discusses related work and Section VII concludes the paper.

II. REVIEW OF AC POWER FLOW

The steady state AC power for bus n is given by

$$\tilde{S}_n = \sum_m^{n \neq m} \tilde{V}_n \tilde{V}_n^* \tilde{Y}_{nm}^* - \tilde{V}_n \tilde{V}_m^* \tilde{Y}_{nm}^*. \quad (1)$$

This equation is not symmetric. From the perspective of bus n , the power flow on a line to bus n is

$$\tilde{V}_n \tilde{V}_n^* \tilde{Y}_{nm}^* - \tilde{V}_n \tilde{V}_m^* \tilde{Y}_{nm}^*$$

while, from the perspective of bus m , it is

$$\tilde{V}_m \tilde{V}_m^* \tilde{Y}_{mn}^* - \tilde{V}_m \tilde{V}_n^* \tilde{Y}_{mn}^*.$$

In general, $\tilde{S}_{nm} \neq \tilde{S}_{mn}$.

A. The Traditional Representation

The AC power flow definition is typically expanded in terms of real numbers only. By representing power in rectangular

form, the real (p_n) and imaginary (q_n) terms become

$$\sum_m^{n \neq m} |\tilde{V}_n|^2 g_{nm} - |\tilde{V}_n| |\tilde{V}_m| (g_{nm} \cos(\theta_n^\circ - \theta_m^\circ) + b_{nm} \sin(\theta_n^\circ - \theta_m^\circ))$$

$$\sum_m^{n \neq m} -|\tilde{V}_n|^2 b_{nm} - |\tilde{V}_n| |\tilde{V}_m| (g_{nm} \sin(\theta_n^\circ - \theta_m^\circ) - b_{nm} \cos(\theta_n^\circ - \theta_m^\circ))$$

The Y-Bus Matrix: The formulation can be simplified further by using a *Y-Bus Matrix*, i.e., a precomputed lookup table that allows the power flow at each bus to be written as a summation of $2n$ terms instead a summation of $3(n-1)$ terms. Observe that, in the power flow equations (1), the first term $\tilde{V}_n \tilde{V}_n^* \tilde{Y}_{nn}^*$ is a special case of the second term $-\tilde{V}_n \tilde{V}_m^* \tilde{Y}_{nm}^*$ with $-\tilde{V}_m = \tilde{V}_n$. We can eliminate this special case by

- 1) extending the summation to include n terms, i.e., $\sum_m^{n \neq m}$ becomes \sum_m ;
- 2) defining the *Y-Bus* admittance \tilde{Y}_{nm}^b as

$$\tilde{Y}_{nn}^b = \sum_m^{n \neq m} \tilde{Y}_{nm}$$

$$\tilde{Y}_{nm}^b = -\tilde{Y}_{nm}$$

Given the Y-Bus, the power flow equations (1) can be rewritten as a single summation

$$\tilde{S}_n = \sum_m \tilde{V}_n \tilde{V}_m^* \tilde{Y}_{nm}^b \quad (2)$$

giving us the popular formulation of active and reactive power:

$$p_n = \sum_m |\tilde{V}_n| |\tilde{V}_m| (g_{nm}^y \cos(\theta_n^\circ - \theta_m^\circ) + b_{nm}^y \sin(\theta_n^\circ - \theta_m^\circ)) \quad (3)$$

$$q_n = \sum_m |\tilde{V}_n| |\tilde{V}_m| (g_{nm}^y \sin(\theta_n^\circ - \theta_m^\circ) - b_{nm}^y \cos(\theta_n^\circ - \theta_m^\circ)) \quad (4)$$

B. An Alternate Representation

The Y-Bus formulation is concise but makes it difficult to reason about the power flow equations. This paper uses the more explicit equations which can be presented as bus and line equations as follows:

$$p_n = \sum_m^{n \neq m} p_{nm} \quad (5)$$

$$q_n = \sum_m^{n \neq m} q_{nm} \quad (6)$$

$$p_{nm} = |\tilde{V}_n|^2 g_{nm} - |\tilde{V}_n| |\tilde{V}_m| g_{nm} \cos(\theta_n^\circ - \theta_m^\circ) - |\tilde{V}_n| |\tilde{V}_m| b_{nm} \sin(\theta_n^\circ - \theta_m^\circ) \quad (7)$$

$$q_{nm} = -|\tilde{V}_n|^2 b_{nm} + |\tilde{V}_n| |\tilde{V}_m| b_{nm} \cos(\theta_n^\circ - \theta_m^\circ) - |\tilde{V}_n| |\tilde{V}_m| g_{nm} \sin(\theta_n^\circ - \theta_m^\circ) \quad (8)$$

Once again, 7 and 8 are asymmetric and the line admittance values Y have not been modified.

C. Extensions for Practical Power Networks

In the above derivation, each line is a conductor with an impedance \tilde{Z} . The formulation can be extended to line charging and other components such as transformers and bus shunts, which are present in nearly all AC system benchmarks. We show how to model these extensions in the Y-Bus formulation for simplicity.

Line Charging: A line connecting buses n and m may have a predefined line charge \tilde{Y}^c . Steady state AC models typically assume that a line charge is evenly distributed across the line and hence it is reasonable to assign equal portions of its charge to both sides of the line. This is incorporated in the Y-Bus matrix as follows:

$$\begin{aligned}\tilde{Y}_{nn}^{b'} &= \tilde{Y}_{nn}^b + \tilde{Y}_{nm}^c/2, \\ \tilde{Y}_{mm}^{b'} &= \tilde{Y}_{mm}^b + \tilde{Y}_{nm}^c/2.\end{aligned}$$

Transformers: A transformer connecting bus n to bus m can be modeled as a line with modifications to the Y-Bus matrix. The properties of the transformer are captured by a complex number $\tilde{T}_{nm} = |\tilde{T}|\angle s^\circ$, where $|\tilde{T}|$ is the tap ratio from n to m and s° is the phase shift. It is worth noting that the direction of a transformer-line is very important to model the tap ratio and phase shift properly. A transformer is modeled in the Y-Bus matrix as follows:

$$\begin{aligned}\tilde{Y}_{nn}^{b'} &= \tilde{Y}_{nn}^b - \tilde{Y}_{nm} + \tilde{Y}_{nm}/|\tilde{T}_{nm}|^2, \\ \tilde{Y}_{nm}^{b'} &= \tilde{Y}_{nm}/\tilde{T}_{nm}^*, \\ \tilde{Y}_{mn}^{b'} &= \tilde{Y}_{mn}/\tilde{T}_{nm}.\end{aligned}$$

If a line charge exists, it must be applied before the transformer calculation, i.e.,

$$\tilde{Y}_{nn}^{b'} = \tilde{Y}_{nn}^b - \tilde{Y}_{nm} + (\tilde{Y}_{nm} + \tilde{Y}_{nm}^c/2)/|\tilde{T}_{nm}|^2$$

Bus Shunts: A bus n may have a shunt element which is modeled as a fixed admittance to ground with a value of \tilde{Y}^s . In the Y-Bus matrix, we have

$$\tilde{Y}_{nn}^{b'} = \tilde{Y}_{nn}^b + \tilde{Y}_n^s$$

Unlike line charging, this extension is not affected by transformers, since it applies to a bus and not a line.

D. The Linearized DC Power Flow

Many variants of the Linearized DC (LDC) model exist [52], [53], [54], [55]. A comprehensive review of all these variants is outside the scope of this work but an in-depth discussion can be found in [47]. For brevity, we only review the simplest and most popular variant of the LDC, which is derived from the AC equations through a series of approximations justified by operational considerations under normal operating conditions. In particular, the LDC assumes that (1) the susceptance is large relative to the conductance $|g| \ll |b|$; (2) the phase angle difference is small enough to ensure $\sin(\theta_n^\circ - \theta_m^\circ) \approx \theta_n^\circ - \theta_m^\circ$; and (3) the voltage magnitudes $|\tilde{V}|$ are close to 1.0 and do not vary significantly. Under these assumptions, Equations (7) and (8) reduce to

$$p_{nm} = -b_{nm}(\theta_n^\circ - \theta_m^\circ) \quad (9)$$

This simple linear formulation has been used in many frameworks for decision support in power systems [15], [18], [31], [41], [45], [46]. This traditional model is used as the baseline in the experimental results.

III. LINEAR-PROGRAMMING APPROXIMATIONS

This section presents linear-programming approximations of the AC power flow equations. To understand the approximations, it is important to distinguish between *hot-start* and *cold-start* contexts [47]. In hot-start contexts, a solved AC base-point solution is available and hence the model has at its disposal additional information such as voltage magnitudes. In cold start contexts, no such solved AC base-point solution is available and it can be "maddeningly difficult" [15] to obtain one by simulation of the network. Hot-start models are well-suited for applications in which the network topology is relatively stable, e.g., in LMP-base market calculations, optimal line switching, distribution configuration, and real-time security constrained economic dispatch. Cold-start models are used when no operational network is available, e.g., in long-term planning studies. We also introduce the concept of *warm-start* contexts, in which the model has at its disposal target voltages (e.g., from normal operating conditions) but an actual solution may not exist for these targets. Warm-start models are particularly useful for power restoration applications in which the goal is to return to normal operating conditions as quickly as possible. This section presents the hot-start, warm-start, and cold-start models in stepwise refinements. It also discusses how models can be generalized to include generation and load shedding, remove the slack bus, impose constraints on voltages and reactive power, and capacity constraints on the lines, all which are fundamental for many applications.

A. AC Power Flow Behavior

Before presenting the models, it is useful to review the behavior of AC power flows, which is the main driver in the derivation. The high-level behavior of power systems is often characterized by two rules of thumb in the literature: (1) phase angles are the primary factor in determining the flow active power; (2) differences in voltage magnitudes are the primary factor in determining the flow of reactive power [56]. We examine these properties experimentally.

The experiments make two basic assumptions: (1) In the per unit system, voltages do not vary far from a magnitude of 1.0 and angle of 0.0; (2) The magnitude of a line conductance is much smaller than the magnitude of the susceptance, i.e., $|g| \ll |b|$. We can then explore the bounds of the power flow equations (7) and (8), when the voltages are in the following bounds: $|\tilde{V}_n| = 1.0$, $|\tilde{V}_m| \in (1.2, 0.8)$, $\theta_n^\circ - \theta_m^\circ \in (-\pi/6, \pi/6)$. These bounds are intentionally generous so that the power flow behavior within and outside normal operating conditions may be illustrated.

Figure 1 presents the contour of the active power (left) and reactive power (right) equations for a line $\langle n, m \rangle$ under these assumptions when $\tilde{Y}_{nm} = 0.2 - i1$. The contour lines indicate significant changes in power flow. Consider first the active power plot (left). For a fixed voltage, varying the phase

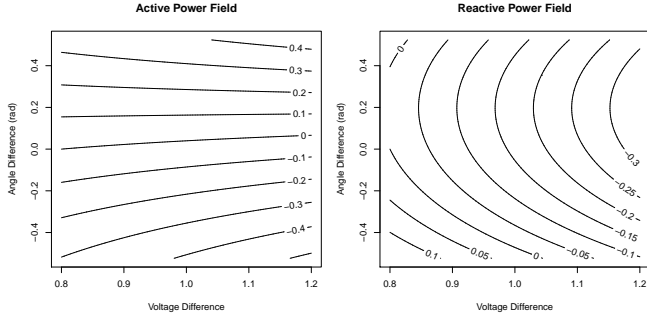


Fig. 1. Power Flow Contour of Active (left) and Reactive (right) Power with $g = 0.2$ and $b = -1$.

angle difference induces significant changes in active power as many lines are crossed. In contrast, for a fixed phase angle difference, varying the voltage has limited impact on the active power, since few lines are crossed. Hence, the plot indicates that phase angle differences are the primary factor of active power flow while voltage differences have only a small effect. The situation is quite different for reactive power (right plot). For a fixed voltage, varying the phase angle difference induces some significant changes in reactive power as around four lines can be crossed. But, if the phase angle difference is fixed, varying voltage induces even more significant changes in reactive power since as many as seven lines may now be crossed. Hence, changes in voltages are the primary factor of reactive power flows but the phase angle differences also have a significant influence.

B. The Hot-Start LPAC Model

The linear-programming approximation of the AC Power flow equations in a hot-start context is based on three ideas:

- 1) It uses the voltage magnitude $|\tilde{V}_n^h|$ from the AC base-point solution at bus n ;
- 2) It approximates $\sin(x)$ by x ;
- 3) It uses a convex approximation of the cosine.¹

Let $\widehat{\cos}(\theta_n^\circ - \theta_m^\circ)$ denote the convexification of $\cos(\theta_n^\circ - \theta_m^\circ)$ in the range $(-\pi/2, \pi/2)$, then the linear-programming approximation solves the line flow constraints

$$\hat{p}_{nm}^h = |\tilde{V}_n^h|^2 g_{nm} - |\tilde{V}_n^h| |\tilde{V}_m^h| g_{nm} \widehat{\cos}(\theta_n^\circ - \theta_m^\circ) - |\tilde{V}_n^h| |\tilde{V}_m^h| b_{nm} (\theta_n^\circ - \theta_m^\circ) \quad (10)$$

$$\hat{q}_{nm}^h = -|\tilde{V}_n^h|^2 b_{nm} + |\tilde{V}_n^h| |\tilde{V}_m^h| b_{nm} \widehat{\cos}(\theta_n^\circ - \theta_m^\circ) - |\tilde{V}_n^h| |\tilde{V}_m^h| g_{nm} (\theta_n^\circ - \theta_m^\circ) \quad (11)$$

The details of the convexification are given in Appendix A. The hot-start model, presented in Model 1, is a linear program that replaces the AC power equations by Equations 10 and 11 and thus captures an approximation of reactive power in a linear formulation.

A complete linear program for this formulation is presented in Model 1. The inputs to the model are: (1) A power network $\mathcal{PN} = \langle N, L, G, s \rangle$, where N is the set of buses, L is the set of lines, G is the set of voltage-controlled generators, s is

¹The domain of the cosine should not exceed the range $(-\pi/2, \pi/2)$ to ensure convexity. This range is generous for AC power flows.

Model 1 The Hot-Start LPAC Model.

Inputs:

- $\mathcal{PN} = \langle N, L, G, s \rangle$ - the power network
- $|\tilde{V}^h|$ - voltage magnitudes from a base-point solution
- cs - cosine approximation segment count

Variables:

- $\theta_n^\circ \in (-\infty, \infty)$ - phase angle on bus n (radians)
- $\widehat{\cos}_{nm} \in (0, 1)$ - Approximation of $\cos(\theta_n^\circ - \theta_m^\circ)$

Maximize:

$$\sum_{\langle n, m \rangle \in L} \widehat{\cos}_{nm} \quad (M1.1)$$

gSubject to:

$$\theta_s^\circ = 0 \quad (M1.2)$$

$$p_n = \sum_{\substack{n \neq m \\ m \in N}} \hat{p}_{nm}^h \quad \forall n \in N \quad n \neq s \quad (M1.3)$$

$$q_n = \sum_{\substack{n \neq m \\ m \in N}} \hat{q}_{nm}^h \quad \forall n \in N \quad n \neq s \quad n \notin G \quad (M1.4)$$

$$\forall \langle n, m \rangle, \langle m, n \rangle \in L \quad \hat{p}_{nm}^h = |\tilde{V}_n^h|^2 g_{nm} - |\tilde{V}_n^h| |\tilde{V}_m^h| (g_{nm} \widehat{\cos}_{nm} + b_{nm} (\theta_n^\circ - \theta_m^\circ)) \quad (M1.5)$$

$$\hat{q}_{nm}^h = -|\tilde{V}_n^h|^2 b_{nm} - |\tilde{V}_n^h| |\tilde{V}_m^h| (g_{nm} (\theta_n^\circ - \theta_m^\circ) - b_{nm} \widehat{\cos}_{nm}) \quad (M1.6)$$

$$\text{PWL}(\text{COS})(\widehat{\cos}_{nm}, (\theta_n^\circ - \theta_m^\circ), -\pi/3, \pi/3, cs) \quad (M1.7)$$

the slack bus; (2) the voltage magnitudes $|V^h|$ for the buses and (3) the number of segments cs for approximating the cosine function. The objective (M1.1) maximizes the cosine approximation to make it as close as possible to the true cosine value. Constraints (M1.2) model the slack bus, which has a fixed phase angle. Constraints (M1.3) and (M1.4) model KCL on the buses. Like in AC power flow models, the KCL constraints are not enforced on the slack bus for both active and reactive power and on voltage-controlled generators for reactive power. Constraints (M1.5) and (M1.6) capture the approximate line flows from Equations (10) and (11). Finally, Constraints (M1.7) define a system of inequalities capturing the piecewise-linear approximation of the cosine terms in the domain $(-\pi/3, \pi/3)$ using cs line segments for each line in the power network.

To our knowledge, this hot-start model is the first linear formulation that captures the cosine contribution to reactive power. However, fixing the voltage magnitudes, $|\tilde{V}^h|$, in the power flow equations may be too restrictive in many applications. In the remaining sections, we remove this restriction.

C. The Warm-Start LPAC Model

This section derives the warm-start LPAC model, i.e., a Linear-Programming model of the AC power flow equations for the warm-start context. The warm-start context assumes that some target voltages $|\tilde{V}^t|$ are available for all buses except voltage-controlled generators whose voltage magnitudes $|\tilde{V}^g|$ are known. The network **must** operate close (e.g., ± 0.1 Volts p.u.) to these target voltages, since otherwise the hardware may be damaged or voltages may collapse.

The warm-start LPAC model is based on two key ideas:

- 1) The active power approximation is the same as in the hot-start model, with the target voltages replacing the voltages in the base-point solution;
- 2) The reactive power approximation reasons about voltage magnitudes, since changes in voltages are the primary factor of reactive power flows.

To derive the reactive power approximation in the warm-start LPAC model, let ϕ be the difference between the target voltage and the true value, i.e.,

$$|\tilde{V}| = |\tilde{V}^t| + \phi.$$

Substituting in Equation 8, we obtain

$$q_{nm} = -(|\tilde{V}_n^t|^2 + 2|\tilde{V}_n^t|\phi_n + \phi_n^2)b_{nm} - (|\tilde{V}_n^t||\tilde{V}_m^t| + |\tilde{V}_n^t|\phi_m + |\tilde{V}_m^t|\phi_n + \phi_n\phi_m)(g_{nm} \sin(\theta_n^\circ - \theta_m^\circ) - b_{nm} \cos(\theta_n^\circ - \theta_m^\circ)) \quad (12)$$

We can divide this expression into two parts

$$q_{nm} = q_{nm}^t + q_{nm}^\Delta \quad (13)$$

where q_{nm}^t is Equation 8 with $|\tilde{V}| = |\tilde{V}^t|$ and q_{nm}^Δ captures the remaining terms, i.e.,

$$q_{nm}^\Delta = -(2|\tilde{V}_n^t|\phi_n + \phi_n^2)b_{nm} - (|\tilde{V}_n^t|\phi_m + |\tilde{V}_m^t|\phi_n + \phi_n\phi_m)(g_{nm} \sin(\theta_n^\circ - \theta_m^\circ) - b_{nm} \cos(\theta_n^\circ - \theta_m^\circ)) \quad (14)$$

Equation 13 is equivalent to Equation 8 and must be linearized to obtain the LPAC model.

The q_{nm}^t part has target voltages and may thus be approximated like \hat{q}_{nm}^h . The q_{nm}^Δ is more challenging as it contains nonlinear and non-convex terms such as $\phi_n\phi_m \cos(\theta_n^\circ - \theta_m^\circ)$. We approximate q_{nm}^Δ using the linear terms of the Taylor series of q_{nm}^Δ at $\phi_n = 0, \phi_m = 0, \theta_n^\circ - \theta_m^\circ = 0$ to obtain

$$\hat{q}_{nm}^\Delta = -(2|\tilde{V}_n^t|\phi_n)b_{nm} + (|\tilde{V}_n^t|\phi_m + |\tilde{V}_m^t|\phi_n)b_{nm} \quad (15)$$

or, equivalently,

$$\hat{q}_{nm}^\Delta = -|\tilde{V}_n^t|b_{nm}(\phi_n - \phi_m) - (|\tilde{V}_n^t| - |\tilde{V}_m^t|)b_{nm}\phi_n \quad (16)$$

A complete linear program for this formulation is presented in Model 2. The inputs to the model are similar to Model 1, with hot start voltages $|\tilde{V}^h|$ replaced by target voltages $|\tilde{V}^t|$. The objective (M2.1) maximizes the cosine approximation to make it as close as possible to the true cosine value. Constraints (M2.2) model the slack bus, which has a fixed voltage and phase angle. Constraints (M2.3) capture the voltage-controlled generators which, by definition, do not vary from their voltage target $|V^t|$. Constraints (M2.4) and (M2.5) model KCL on the buses, as well as the effects of voltage change presented in Equation (16). Like in AC power flow models, the KCL constraints are not enforced on the slack bus for both active and reactive power and on voltage-controlled generators for reactive power. Constraints (M2.6) and (M2.7) capture the approximate line flows from Equations (10) and (11). Constraints (M2.8) model the effects of voltage change presented in Equation (16). Finally, Constraints (M2.9) define a system of inequalities capturing the piecewise-linear approximation of the cosine terms in the domain $(-\pi/3, \pi/3)$ using cs line segments for each line in the power network.

Model 2 The Warm-Start LPAC Model.

Inputs:

- $\mathcal{PN} = \langle N, L, G, s \rangle$ - the power network
- $|\tilde{V}^t|$ - target voltage magnitudes
- cs - cosine approximation segment count

Variables:

- $\theta_n^\circ \in (-\infty, \infty)$ - phase angle on bus n (radians)
- $\phi_n \in (-|\tilde{V}^t|, \infty)$ - voltage change on bus n (Volts p.u.)
- $\widehat{cos}_{nm} \in (0, 1)$ - Approximation of $\cos(\theta_n^\circ - \theta_m^\circ)$

Maximize:

$$\sum_{(n,m) \in L} \widehat{cos}_{nm} \quad (M2.1)$$

Subject to:

$$\theta_s^\circ = 0, \phi_s = 0 \quad (M2.2)$$

$$\phi_i = 0 \quad \forall i \in G \quad (M2.3)$$

$$p_n = \sum_{\substack{m \in N \\ m \neq n}} \hat{p}_{nm}^t \quad \forall n \in N \quad n \neq s \quad (M2.4)$$

$$q_n = \sum_{\substack{m \in N \\ m \neq n}} \hat{q}_{nm}^t + \hat{q}_{nm}^\Delta \quad \forall n \in N \quad n \neq s \quad n \notin G \quad (M2.5)$$

$$\forall (n, m), (m, n) \in L$$

$$\hat{p}_{nm}^t = |\tilde{V}_n^t|^2 g_{nm} - |\tilde{V}_n^t||\tilde{V}_m^t|(g_{nm}\widehat{cos}_{nm} + b_{nm}(\theta_n^\circ - \theta_m^\circ)) \quad (M2.6)$$

$$\hat{q}_{nm}^t = -|\tilde{V}_n^t|^2 b_{nm} - |\tilde{V}_n^t||\tilde{V}_m^t|(g_{nm}(\theta_n^\circ - \theta_m^\circ) - b_{nm}\widehat{cos}_{nm}) \quad (M2.7)$$

$$\hat{q}_{nm}^\Delta = -|\tilde{V}_n^t|b_{nm}(\phi_n - \phi_m) - (|\tilde{V}_n^t| - |\tilde{V}_m^t|)b_{nm}\phi_n \quad (M2.8)$$

$$\text{PWL}(COS)(\widehat{cos}_{nm}, (\theta_n^\circ - \theta_m^\circ), -\pi/3, \pi/3, cs) \quad (M2.9)$$

D. The Cold-Start LPAC Model

We now conclude by presenting the cold-start LPAC model. In a cold-start context, no target voltages are available and voltage magnitudes are approximated by 1.0, except for voltage-controlled generators whose voltages are given by $|\tilde{V}_n^g|$ ($n \in G$). The cold-start LPAC model is then derived from the warm-start LPAC model by fixing $|\tilde{V}_i^t| = 1$ for all $i \in N$. Equation (16) then reduces to

$$\hat{q}_{nm}^\Delta = -b_{nm}(\phi_n - \phi_m) \quad (17)$$

Figure 3 presents the cold-start LPAC model, which is very close to the warm-start model. Note that Constraints (M3.3) use ϕ_i to fix the voltage magnitudes of generators.

E. Extensions to the LPAC Model

The LPAC models can be used to solve the AC power flow equations approximately in a variety of contexts. This section reviews how to generalize the LPAC models for applications in disaster management, reactive voltage support, transmission planning, and vulnerability analysis. The extensions are illustrated on the warm-start model but can be similarly applied to the cold-start model.

Generators: The LPAC model can easily be generalized to include ranges for generators: Simply remove the generator from G and place operating limits on the p and q variables for that bus. In this formulation, voltage-controlled generators can also be accommodated by fixing ϕ_n to zero at bus n .

Removing the Slack Bus: By necessity, AC solvers use a slack bus to ensure the flow balance in the network when the total power consumption is not known a priori (e.g., due to line losses). As a consequence, the LPAC model depicted in Figure 2 also uses a slack bus so that the AC and LPAC models can be accurately compared in our experimental results. However, it is important to emphasize that the LPAC model does not

Model 3 The Cold-Start LPAC Model.

Inputs:

$\mathcal{PN} = \langle N, L, G, s \rangle$ - the power network
 cs - cosine approximation segment count

Variables:

$\theta_n^\circ \in (-\infty, \infty)$ - phase angle on bus n (radians)
 $\phi_n \in (-|V_n^t|, \infty)$ - voltage change on bus n (Volts p.u.)
 $\widehat{cos}_{nm} \in (0, 1)$ - Approximation of $\cos(\theta_n^\circ - \theta_m^\circ)$

Maximize:

$$\sum_{\langle n, m \rangle \in L} \widehat{cos}_{nm} \quad (M3.1)$$

Subject to:

$$\theta_s^\circ = 0, \phi_s = |\widetilde{V}_s^g| - 1.0 \quad (M3.2)$$

$$\phi_i = |\widetilde{V}_i^g| - 1.0 \quad \forall i \in G \quad (M3.3)$$

$$p_n = \sum_{\substack{m \in N \\ n \neq m}} \hat{p}_{nm}^t \quad \forall n \in N \quad n \neq s \quad (M3.4)$$

$$q_n = \sum_{\substack{m \in N \\ n \neq m}} \hat{q}_{nm}^t + \hat{q}_{nm}^\Delta \quad \forall n \in N \quad n \neq s \quad n \notin G \quad (M3.5)$$

$$\forall \langle n, m \rangle, \langle m, n \rangle \in L \quad (M3.6)$$

$$\hat{p}_{nm}^t = g_{nm} - g_{nm} \widehat{cos}_{nm} - b_{nm}(\theta_n^\circ - \theta_m^\circ) \quad (M3.7)$$

$$\hat{q}_{nm}^t = -b_{nm} - g_{nm}(\theta_n^\circ - \theta_m^\circ) + b_{nm} \widehat{cos}_{nm} \quad (M3.8)$$

$$\hat{q}_{nm}^\Delta = -b_{nm}(\phi_n - \phi_m) \quad (M3.9)$$

$$\text{PWL}(COS)(\widehat{cos}_{nm}, (\theta_n^\circ - \theta_m^\circ), -\pi/3, \pi/3, cs) \quad (M3.9)$$

need a slack bus and the only reason to include a slack bus in this model is to allow for meaningful comparisons between the LPAC and AC models. As discussed above, the LPAC model can easily include a range for each generator, thus removing the need for a slack bus.

Load Shedding: For applications in power restoration (e.g., [45], [46], [51]), the LPAC model can also integrate load shedding: Simply transform the loads into decision variables with an upper bound and maximize the load served. The cosine maximization should also be included in the objective but with a smaller weight. Section V-A reports experimental results on such a power restoration model.

Modeling Additional Constraints: In practice, feasibility constraints may exist on the acceptable voltage range, the reactive injection of a generator, or line flow capacities. Because Model 2 is a linear program, it can incorporate such constraints. For instance, constraint

$$\underline{|V|} \leq |V_n^t| + \phi_n \quad \forall n \in N$$

ensures that voltages are above a certain limit $\underline{|V|}$, constraint

$$\sum_{\substack{n \neq m \\ m \in N}} \hat{q}_{nm}^t + \hat{q}_{nm}^\Delta \leq \overline{q_n} \quad \forall n \in G$$

limits the maximum reactive injection bounds at bus n to $\overline{q_n}$. Finally, let $\overline{|S_{nm}|}$ be the maximum apparent power on a line from bus n to bus m . Then, constraint

$$(\hat{p}_{nm}^t)^2 + (\hat{q}_{nm}^t + \hat{q}_{nm}^\Delta)^2 \leq \overline{|S_{nm}|}^2$$

ensures that line flows are feasible in the LPAC model. The quadratic functions can be approximated by piecewise-linear constrains (e.g., [50]).

IV. ACCURACY OF THE LPAC MODEL

This section evaluates the accuracy of the LPAC models by comparing them to an ideal nonlinear AC power flow.² It includes a detailed analysis of the model accuracy (Section IV-A) and an investigation of alternative approximations (Section IV-B). The experiments were performed on nine traditional power-system benchmarks which come from the IEEE test systems [57] and MATPOWER [58]. The AC power flow equations were solved with a Newton-Raphson solver which was validated using MATPOWER. The LPAC models use 20 line segments in the cosine approximation and all of the models solved in less than 1 second on a 2.5 GHz Intel processor. The results also include a modified version of the IEEE118 benchmark, called IEEE118m. The original IEEE118 has the slack bus connected to the network by a transformer with $|\widetilde{T}| = 1.05$. The nonlinear behavior of transformers induces some loss of accuracy in the LPAC model and, because this error occurs at the slack bus in IEEE118, it affects all buses in the network. IEEE118m resolves this issue by setting $|\widetilde{T}| = 1.00$ and the slack bus voltage to 1.05. As the results indicate, this equivalent formulation is significantly better for the LPAC model.

A. Accuracy of The LPAC Models

This section reports empirical evaluations of the LDC and LPAC models in cold-start and warm-start contexts. It reports aggregate statistics for active power (Table I), bus phase angles (Table II), reactive power (Table III), and voltage magnitudes (Table IV). Data for the LDC model is necessarily omitted from Tables III and IV as reactive power and voltages are not captured by that model. In each table, two aggregate values are presented: Correlation (corr) and absolute error (Δ). The units of the absolute error are presented in the headings. Both average (μ) and worst-case (max) values are presented. The worst case can often be misleading: For example a very large value may actually be a very small relative quantity. For this reason, the tables show the relative error (δ) of the value selected by the max operator using the arg-max operator. The relative error is a percentage and is unit-less.

Table I indicates uniform improvements in active power flows, especially in the largest benchmarks IEEE118, IEEE118m, and MP300. Significant errors are not uncommon for the linearized DC model on large benchmarks [47] and are primarily caused by a lack of line losses. Due to its asymmetrical power flow equations and the cosine approximation, the LPAC model captures line losses.

Table II presents the aggregate statistics on bus phase angles. These results show significant improvements in accuracy especially on larger benchmarks. The correlations are somewhat lower than active power, but phase angles are quite challenging from a numerical accuracy standpoint.

Table III presents the aggregate statistics on line reactive power flows. They indicate that reactive power flows are generally accurate and highly precise in warm-start contexts. To highlight the model accuracy in cold-start contexts, the reactive

²For consistency, the LPAC models are extended to include line charging, bus shunts, and transformers, as discussed in Section II-C.

TABLE I
ACCURACY OF THE LPAC MODEL: ACTIVE POWER FLOWS.

Benchmark	Active Power (MW)			
	Corr	$\mu(\Delta)$	$\max(\Delta)$	$\delta(\arg\text{-max}(\Delta))$
The LDC Model				
ieee14	0.9994	1.392	10.64	6.783
mp24	0.9989	5.659	19.7	23.65
ieee30	0.9993	1.046	13.1	7.562
mp30	0.9993	0.2964	2.108	19.36
mp39	0.9995	7.341	43.64	6.527
ieee57	0.9989	1.494	8.216	8.055
ieee118	0.9963	3.984	56.3	44.74
ieeedd17	0.9972	4.933	201.3	13.84
ieeedd17m	0.9975	4.779	191.1	13.23
mp300	0.9910	11.09	418.5	90.02
The LPAC-Cold Model				
ieee14	0.9989	1.636	5.787	13.13
mp24	0.9999	1.884	6.159	2.933
ieee30	0.9998	0.5475	2.213	2.523
mp30	0.9995	0.2396	1.641	15.07
mp39	1.0000	2.142	8.043	3.288
ieee57	0.9995	0.9235	4.674	9.728
ieee118	1.0000	0.622	3.708	2.038
ieeedd17	0.9999	1.827	30.38	2.088
ieeedd17m	0.9999	1.475	20.21	1.399
mp300	0.9998	2.455	18	8.675
The LPAC-Warm Model				
ieee14	1.0000	0.1689	1.588	1.012
mp24	1.0000	0.6621	2.041	1.01
ieee30	1.0000	0.1847	2.433	1.405
mp30	0.9999	0.1052	0.705	6.474
mp39	1.0000	1.557	11.58	1.731
ieee57	1.0000	0.2229	2.013	1.973
ieee118	0.9999	0.4386	7.376	5.862
ieeedd17	1.0000	0.58	22.5	1.547
ieeedd17m	1.0000	0.5725	21.73	1.504
mp300	0.9999	1.195	52.84	11.37

TABLE II
ACCURACY OF THE LPAC MODEL: PHASE ANGLES.

Benchmark	Phase Angle (rad)			
	Corr	$\mu(\Delta)$	$\max(\Delta)$	$\delta(\arg\text{-max}(\Delta))$
The LDC Model				
ieee14	0.9993	0.02487	0.04258	15.22
mp24	0.9997	0.01334	0.02037	15.23
ieee30	0.9981	0.02831	0.04733	16.45
mp30	0.9800	0.005658	0.01607	30.27
mp39	0.9951	0.0283	0.05813	85.56
ieee57	0.9898	0.02244	0.05958	24.1
ieee118	0.9904	0.03452	0.09026	88.41
ieeedd17	0.9892	0.115	0.1395	16.09
ieeedd17m	0.9920	0.0461	0.06924	41.88
mp300	0.9752	0.3103	0.4244	975.7
The LPAC-Cold Model				
ieee14	0.9971	0.004525	0.01241	5
mp24	0.9999	0.003539	0.008947	6.922
ieee30	0.9965	0.007268	0.02413	8.386
mp30	0.9782	0.006236	0.01804	33.99
mp39	0.9989	0.006268	0.02314	34.06
ieee57	0.9894	0.0179	0.05467	22.11
ieee118	0.9994	0.003225	0.01354	9.633
ieeedd17	0.9981	0.03648	0.05165	5.958
ieeedd17m	0.9990	0.007207	0.02682	4.522
mp300	0.9984	0.01458	0.08086	38.49
The LPAC-Warm Model				
ieee14	1.0000	0.001448	0.001829	0.6914
mp24	1.0000	0.001337	0.002203	2.156
ieee30	1.0000	0.002345	0.002819	0.9629
mp30	0.9998	0.001298	0.001774	4.775
mp39	0.9999	0.005315	0.006241	4.273
ieee57	1.0000	0.002711	0.00357	1.776
ieee118	0.9999	0.005958	0.008366	2.526
ieeedd17	0.9999	0.01492	0.01719	2.419
ieeedd17m	0.9999	0.008443	0.01059	2.33
mp300	0.9997	0.03842	0.04502	18.51

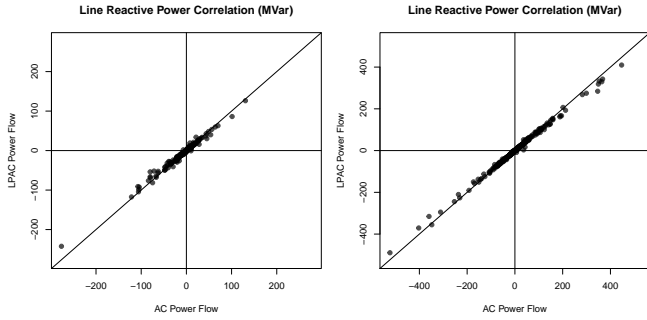


Fig. 2. Reactive Power Flow Correlation for the LPAC Model on IEEEEd17m (left) and MP300 (right) in a cold-start context.

flow correlation for the two worst benchmarks, IEEEEd17m and MP300, is presented in Figure 2.

Table IV presents the aggregate statistics on bus voltage magnitudes. These results indicate that voltage magnitudes are very accurate on small benchmarks, but the accuracy reduces with the size of the network. The warm-start context brings a significant increase in accuracy in larger benchmarks. To illustrate the quality of these solutions in cold-start contexts, the voltage magnitude correlation for the two worst benchmarks, i.e., IEEEEd17m and MP300, is presented in Figure 3. The increase in voltage errors is related to the distance from a load point to the nearest generator. The linearized voltage model incurs some small error on each line. As the voltage changes

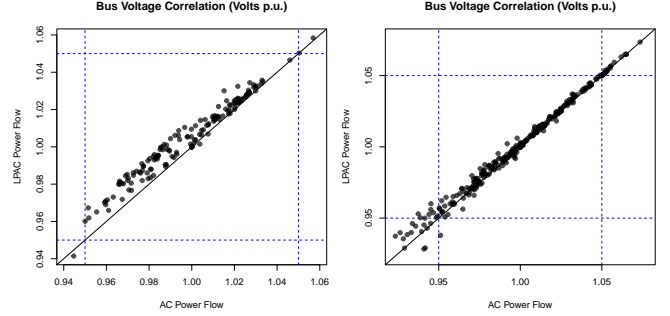


Fig. 3. Voltage magnitude correlation for Model LPAC on IEEEEd17m (left) and MP300 (right) in a cold-start context.

over many lines, these small errors accumulate. By comparing the percentage of voltage-controlled generator buses in each benchmark $|G|/|N|$ (Table V) to accuracy in Table IV, the IEEE57 and IEEEEd17 benchmarks indicate that a low percentage is a reasonable indicator of the voltage accuracy in the cold-start context.

B. Alternative Linear Models

The formulation of the LPAC models explicitly removes two core assumptions of the traditional LDC model:

- 1) Although $\cos(\theta_n^\circ - \theta_m^\circ)$ maybe very close to 1, those small deviations are important.

TABLE III
ACCURACY OF THE LPAC MODEL: REACTIVE POWER FLOWS.

Benchmark	Corr	Reactive Power (MVar)		
		$\mu(\Delta)$	$\max(\Delta)$	$\delta(\arg\text{-max}(\Delta))$
The LPAC-Cold Model				
ieee14	0.9948	0.7459	2.561	14.92
mp24	0.9992	1.505	5.245	9.309
ieee30	0.997	0.4962	1.902	23.36
mp30	0.9991	0.3135	0.8925	3.886
mp39	0.9973	3.898	15.15	18.25
ieee57	0.9991	0.5316	2.98	3.973
ieee118	0.9991	0.7676	6.248	8.561
ieeedd17	0.9789	3.989	48.65	40.58
ieeedd17m	0.9927	2.415	34.18	12.36
mp300	0.9981	3.85	62.32	17.98
The LPAC-Warm Model				
ieee14	0.9895	0.8689	3.167	43.89
mp24	0.9992	1.505	5.245	9.309
ieee30	0.9975	0.3455	1.607	7.62
mp30	0.9991	0.3135	0.8925	3.886
mp39	0.9971	4.03	15.75	18.98
ieee57	0.9995	0.3853	1.46	5.67
ieee118	0.9992	0.6326	6.109	6.808
ieeedd17	0.9791	3.985	48.37	40.34
ieeedd17m	0.9927	2.409	33.96	12.28
mp300	0.9943	3.584	162	45.05

TABLE IV
ACCURACY OF THE LPAC MODEL: VOLTAGE MAGNITUDES.

Benchmark	Corr	Voltage Magnitude (Volts p.u.)		
		$\mu(\Delta)$	$\max(\Delta)$	$\delta(\arg\text{-max}(\Delta))$
The LPAC-Cold Model				
ieee14	0.9828	0.003524	0.01304	1.236
mp24	0.9983	0.000676	0.003244	0.3362
ieee30	0.9908	0.002445	0.01098	1.098
mp30	0.9884	0.002186	0.009453	0.9723
mp39	0.9992	0.0007521	0.002446	0.2313
ieee57	0.9726	0.01038	0.03353	3.587
ieee118	0.9989	0.000717	0.00476	0.4926
ieeedd17	0.9651	0.01376	0.03345	3.424
ieeedd17m	0.9815	0.00647	0.01579	1.659
mp300	0.9948	0.002361	0.01552	1.656
The LPAC-Warm Model				
ieee14	0.9998	0.0005479	0.001173	0.1111
mp24	0.9996	0.000542	0.002214	0.2294
ieee30	0.9994	0.001426	0.002508	0.25
mp30	1.0000	0.0003884	0.000707	0.073
mp39	0.9983	0.00154	0.003545	0.3524
ieee57	0.9987	0.002138	0.005515	0.59
ieee118	0.9999	0.0001961	0.001303	0.1344
ieeedd17	0.9858	0.01204	0.02597	2.796
ieeedd17m	0.9760	0.009819	0.02037	2.067
mp300	0.9967	0.002477	0.01403	1.52

- 2) Although $|g| \ll |b|$, the conductance contributes significantly to the phase angles and voltage magnitudes.

This section investigates three variants of the cold-start LPAC model that reintegrate some of the assumptions of the LDC model. The new models are: (1) the LPAC-C model where only the cosine approximation is used and $g = 0$; (2) the LPAC-G model where only the g value is used and $\cos(x) = 1$; (3) the LPAC-CG model where $\cos(x) = 1$ and $g = 0$. Tables VI and VII present the *cumulative absolute error* between the proposed linear formulations and the true nonlinear solutions. Many metrics may be of interest but these results focus on line voltage drop $\tilde{V}_n - \tilde{V}_m$ and bus power \tilde{S}_n . These were selected because they are robust to errors which accumulate as power flows through the network. The results highlight

TABLE V
PERCENTAGE OF VOLTAGE-CONTROLLED BUSES IN THE BENCHMARKS.

ieee14	mp24	ieee30	mp30	mp39
35.7%	45.8%	20.0%	20.0%	30.8%
ieee57	ieee118	ieeedd17	mp300	
12.3%	45.8%	7.4%	24.7%	

TABLE VI
ACCURACY COMPARISON OF VARIOUS LINEAR MODELS (PART I).

Model	Cumulative Absolute Error			
	$\Re(\tilde{V}_n - \tilde{V}_m)$	$\Im(\tilde{V}_n - \tilde{V}_m)$	p_n	q_n
ieee14				
LDC	0.3839	0.166	13.39	118.4
LPAC-A-GC	0.1561	0.1296	13.39	140.7
LPAC-A-G	0.1221	0.1229	13.39	120.7
LPAC-A-C	0.1277	0.1262	8.843	53.24
LPAC	0.1008	0.1234	1.783	11.43
mp24				
LDC	0.448	0.1434	53.22	792.4
LPAC-A-GC	0.3676	0.1289	53.22	546.2
LPAC-A-G	0.2309	0.1332	53.22	314.3
LPAC-A-C	0.2417	0.116	53.12	476.2
LPAC	0.03411	0.0828	6.94	64.12
ieee30				
LDC	0.5429	0.2934	17.55	169.9
LPAC-A-GC	0.1607	0.2377	17.55	173.8
LPAC-A-G	0.1284	0.2268	17.55	147.7
LPAC-A-C	0.1587	0.1638	15.99	66.28
LPAC	0.1305	0.1476	2.9	16.72
mp30				
LDC	0.4341	0.1728	2.444	181
LPAC-A-GC	0.166	0.1584	2.444	20.78
LPAC-A-G	0.1616	0.1581	2.444	17.96
LPAC-A-C	0.06886	0.1454	2.444	9.387
LPAC	0.07338	0.1456	1.736	6.76
mp39				
LDC	0.5634	0.1997	43.64	2816
LPAC-A-GC	0.2449	0.2105	43.64	950.3
LPAC-A-G	0.1418	0.1958	43.64	284.1
LPAC-A-C	0.1896	0.1868	37.65	947.9
LPAC	0.04462	0.1337	0.4745	93.31

two interesting points. First, all linear models tend to bring improvements over a traditional LDC model. Second, although integrating either the g value or the cosine term brings some small improvement independently, together they make significant improvements in accuracy. Additionally a comparison of Table VI and Table VII reveals that the benefits of the new linear models are more pronounced as the network increases.

V. CASE STUDIES

This section describes two case studies to evaluate the potential of the LPAC models: Power restoration and capacitor placement. The goal is not to present comprehensive solutions for these two complex problems, but to provide preliminary evidence that the LPAC models may be useful in striking a good compromise between efficiency and accuracy for such applications. This section should be viewed as presenting a “proof-of-concept” that the LPAC models may be valuable for certain classes of applications where the LDC model is not accurate enough and existing approaches are too time consuming or suboptimal.

TABLE VII
ACCURACY COMPARISON OF VARIOUS LINEAR MODELS (PART II).

Model	Cumulative Absolute Error			
	$\Re(\tilde{V}_n - \tilde{V}_m)$	$\Im(\tilde{V}_n - \tilde{V}_m)$	p_n	q_n
ieee57				
LDC	1.343	0.6803	27.9	529.1
LPAC-A-GC	0.4158	0.5489	27.9	264
LPAC-A-G	0.3238	0.5311	27.9	264.1
LPAC-A-C	0.3773	0.4153	24.43	113.8
LPAC	0.3647	0.3854	4.736	26.35
ieee118				
LDC	3.083	1.239	132.7	2152
LPAC-A-GC	0.7298	0.9944	132.7	1364
LPAC-A-G	0.6502	0.9929	132.7	1194
LPAC-A-C	0.4417	0.8553	104.3	750
LPAC	0.2625	0.5252	0.7279	142.1
ieeedd17				
LDC	4.144	3.263	201.3	3857
LPAC-A-GC	5.783	4.881	201.3	2719
LPAC-A-G	4.169	3.242	201.3	616.4
LPAC-A-C	4.162	3.48	200.5	2660
LPAC	1.135	1.019	30.38	362.1
ieeedd17m				
LDC	3.798	1.972	191.1	3353
LPAC-A-GC	5.152	3.219	191.1	2210
LPAC-A-G	3.302	2.111	191.1	389.4
LPAC-A-C	3.31	2.118	190.4	2146
LPAC	0.49	0.6324	20.21	223.7
mp300				
LDC	13.76	4.689	418.5	14240
LPAC-A-GC	11.2	5.324	418.5	5595
LPAC-A-G	9.831	5.171	418.5	1648
LPAC-A-C	7.855	4.403	348.5	5434
LPAC	0.8699	1.378	9.703	976.4

A. Power Restoration

After a significant disruption due to, say, a natural disaster, large sections of the power network need to be re-energized. To understand the effects of restoration actions, power engineers must simulate the network behaviour under various courses of action. However, the network is far from its normal operating state, which makes it extremely challenging to solve the AC power flow equations. In fact, the task of finding an AC solution without a reasonable starting point has been regarded as "maddeningly difficult" [15]. The LPAC model studied here has the benefit of providing starting values for all the variables in the AC power flow problem, unlike the traditional LDC which only provides active power values. Furthermore, the LPAC model has the additional advantage of supporting bounds on reactive generation and voltage magnitudes and such constraints are critical for providing feasible solutions to the AC power flow. This section illustrates these benefits.

Before presenting the power-restoration model, it is important to mention the key aspect of this application. When the power system undergoes significant damages, load shedding must occur. The LDC and LPAC models must be embedded in a restoration model that maximizes the served load given operational constraints such as the generation limits. These load values indicate the maximum amount of power that can be dispatched while ensuring system stability. Model 4 presents a linear program based on the warm-start LPAC model which, given limits on active power generation \bar{p}^g and the desired active and reactive loads \bar{p}^l, \bar{q}^l at each bus, determines the

Model 4 A LP for Maximizing Desired Load.

Inputs:

- \bar{p}_n^g - maximum active injection for bus n
- \bar{p}_n^l - desired active load at bus n
- \bar{q}_n^l - desired reactive load at bus n

Inputs from Model 2 (The Warm-Start LPAC Model)

Variables:

- $p_n^g \in (0, \bar{p}_n^g)$ - active generation at bus n
- $q_n^g \in (-\infty, \infty)$ - reactive generation at bus n
- $l_n \in (0, 1)$ - percentage of load served at bus n

Variables from Model 2 (The Warm-Start LPAC Model)

Maximize:

$$\sum_{n \in N} l_n \quad (\text{M4.1})$$

Subject to:

$$p_n = -\bar{p}_n^l l_n + p_n^g \quad \forall n \in N \quad (\text{M4.2})$$

$$q_n = -\bar{q}_n^l l_n + q_n^g \quad \forall n \in N \quad (\text{M4.3})$$

$$q_n^g = 0 \quad \forall n \in N \setminus G \quad (\text{M4.4})$$

$$q_n = \sum_{m \in N, m \neq n} \hat{q}_{nm}^t + \hat{q}_{nm}^\Delta \quad \forall n \in G \quad (\text{M4.5})$$

Constraints from Model 2 (The Warm-Start LPAC Model)

maximum amount of load that can be dispatched. The model assumes that the loads can be shed continuously and that the active and reactive parts of the load should maintain the same power factor. The objective function (M4.1) maximizes the percentage of served load. Constraints (M4.2) and (M4.3) set the active and reactive injection at bus n appropriately based on the decision variables for load shedding and generation dispatch. Constraint (M4.4) ensures that reactive generation only occurs at generator buses and Constraint (M4.5) now defines q_n for generator buses as well.

Since it reasons about reactive power and voltage magnitudes, Model 4 can be further enhanced to impose bounds on these values. As we will show, such bounds are often critical to obtain high-quality solutions in power restoration contexts. If a reactive generation bound \bar{q}^g is supplied, this model can be extended by adding the constraint,

$$q_n^g \leq \bar{q}_n^g \quad \forall n \in N.$$

Voltage magnitude limits can also be incorporated. Given upper and lower voltage limits $|\tilde{V}|$ and $|\underline{\tilde{V}}|$, the constraint

$$|\underline{\tilde{V}}| \leq 1.0 + \phi_n \leq |\tilde{V}| \quad \forall n \in N.$$

may be used to enforce bounds on voltage magnitudes. The experimental results study the benefits of the LPAC model, suitably enhanced to capture these extensions, for power restoration. They compare a variety of linear models including the LDC model, the LPAC model, and enhancements of the LPAC model with additional constraints on reactive power and voltage magnitudes.

Table VIII studies the applicability of various linear power models for network restoration on the IEEE30 benchmark. 1000 line outage cases were randomly sampled from each of the $N-3, N-4, N-5, \dots, N-20$ contingencies. Each contingency is solved with a linear power model (e.g., the LDC model or the LPAC model), whose solution is used as a starting point for the AC model. The performance metric

TABLE VIII
POWER RESTORATION: ACHIEVING AC FEASIBILITY FROM DIFFERENT MODELS.

Scenario	LDC	LPAC	LPAC-R	LPAC-R-V
$N-3$	998	999	1000	1000
$N-4$	999	1000	1000	1000
$N-5$	987	994	1000	1000
$N-6$	507	594	903	1000
$N-7$	738	856	973	974
$N-8$	949	996	1000	1000
$N-9$	847	932	1000	1000
$N-10$	219	452	992	999
$N-11$	726	972	1000	997
$N-12$	491	779	998	999
$N-13$	444	617	983	991
$N-14$	545	637	998	1000
$N-15$	1000	1000	1000	1000
$N-16$	989	1000	1000	1000
$N-17$	1000	1000	1000	1000
$N-18$	969	1000	1000	1000
$N-19$	999	1000	1000	1000
$N-20$	1000	1000	1000	1000

TABLE IX
POWER RESTORATION: AVERAGE LOAD SHEDDING (% OF TOTAL ACTIVE POWER).

Scenario	LDC	LPAC	LPAC-R	LPAC-R-V
$N-3$	3.23	6.193	15.94	15.99
$N-4$	2.827	3.55	9.183	9.278
$N-5$	0.9562	2.204	8.027	8.082
$N-6$	5.805	6.149	9.287	9.921
$N-7$	1.506	5.709	19.43	19.46
$N-8$	13.78	18.54	27.37	27.39
$N-9$	15.92	24.27	42.76	42.78
$N-10$	29.23	24.02	32.09	32.25
$N-11$	25.18	25.24	42.62	42.63
$N-12$	36.35	28.25	38.03	38.82
$N-13$	40.1	32.56	38.3	38.66
$N-14$	39.98	36.9	40.45	40.67
$N-15$	81.91	81.92	81.92	81.92
$N-16$	86.21	86.31	86.32	86.32
$N-17$	89.89	89.89	89.89	89.89
$N-18$	88.26	88.3	88.32	88.32
$N-19$	85.9	86.13	86.13	86.13
$N-20$	86.2	86.37	86.38	86.38

is the number of cases where the AC solver converges, as a good linear model should yield a feasible generation dispatch with a good starting point for the AC solver. To understand the importance of various network constraints, four linear models are studied: the traditional LDC model; the LPAC model; the LPAC model with constraints on reactive generation (LPAC-R); and the LPAC with constraints on reactive generation and voltage limits (LPAC-R-V). The number of solved models for each of the contingency classes is presented in Table VIII. The results indicate that a traditional LDC model is overly optimistic and often produces power dispatches that do not lead to feasible AC power flows (the $N-10$ and $N-13$ are particularly striking). However, each refinement of the LPAC model solves more contingencies. The LPAC-R-V model is very reliable and is able to produce feasible dispatches in all contingencies except 40. This means that the LPAC-R-V model solves 99.76% of the 17,000 contingencies studied. Table IX depicts the load shed by the various models. For large contingencies, the LPAC-R-V model not only provides good starting points for an AC solver but its load shedding is only

slightly larger than the (overly optimistic) LDC model. These results provide compelling evidence of the benefits of the LPAC model for applications dealing with situations outside the normal operating conditions. In addition, Model 4 can replace the LDC model in power restoration applications (e.g., [45], [46]) that are using MIP models to minimize the size of a blackout over time.

B. The Capacitor Placement Problem

The Capacitor Placement Problem (CPP) is a well-studied application [28], [29], [30] and many variants of the problem exist. This section uses a simple version of the problem to demonstrate how the LPAC model can be used as a building block inside a MIP solver for decision-support applications.

Informally speaking, the CPP consists of placing capacitors throughout a power network to improve voltage stability. The version studied here aims at placing as few capacitors as possible throughout the network, while meeting a lower bound $|\underline{V}|$ on the voltages and satisfying a capacitor injection limit \bar{q}^c and reactive generation limits \bar{q}_n^g ($n \in G$). Model 5 presents a CPP model based on the *cold-start* LPAC model. For each bus n , the additional decision variables are the amount of reactive support added by the capacitor q_n^c and a variable c_n indicating whether a capacitor was used.

The objective function (M5.1) minimizes the number of capacitors. Constraints (M5.2) ensure the voltages do not drop below the desired limit and do not exceed the preferred operating condition of 1.05 Volts p.u. Constraints (M5.3) link the capacitor injection variables with the indicator variables, a standard technique in MIP models. Constraints (M5.4) ensures each generator $n \in G$ does not exceed its reactive generation limit \bar{q}_n^g . and constraints (M5.5) defines the reactive power for generators. Lastly, Constraints (M5.6) redefines the reactive power equation to inject the capacitor contribution q^c . The remainder of the model is the same as Model 3 (the cold-start LPAC model).

The CPP model was tested on a modified version of the IEEE57 benchmark. All of the IEEE benchmarks have sufficient reactive support in their normal state. To make an interesting capacitor placement problem, the transformer tap ratios are set to 1.0 and existing synchronous condensers are removed. This modified benchmark (IEEE57-C) has significant voltage problems with several bus voltages dropping below 0.9. By design, a solution to Model 5 satisfies all of the desired constraints. However, Model 5 is based on the LPAC model and is only an approximation of the AC power flow. To understand the *true* value of Model 5, we solve the resulting solution network with an AC solver and measure how much the constraints are violated. Table X presents the results of Model 5 on benchmark IEEE57-C with $\bar{q}^c = 30$ and various thresholds $|\underline{V}|$. The table presents the following quantities: The minimum desired voltage $|\underline{V}|$; The worst violation of the voltage lower-bound $\min(|\underline{V}|)$; The worst violation of the voltage upper bound $\max(|\underline{V}|)$; The worst violation of reactive injection upper bound $\max(q_n)$; The number of capacitors placed $\sum c_n$; and the runtime of the MIP to prove the optimal placement solution. The table indicates that the CPP model is

Model 5 A MIP for the Capacitor Placement Problem.

Inputs:

\bar{q}_n^g	- injection bound for generator n
\bar{q}_n^c	- capacitor injection bound
$ \underline{\tilde{V}} $	- minimum desired voltage magnitude

Inputs from Model 3 (The Cold-Start LPAC Model)

Variables:

$q_n^c \in (0, \bar{q}_n^c)$	- capacitor reactive injection
$c_n \in \{0, 1\}$	- capacitor placement indicator

Variables from Model 3 (The Cold-Start LPAC Model)

Minimize:

$$\sum_{n \in N} c_n \quad (\text{M5.1})$$

Subject to:

$$|\underline{\tilde{V}}| \leq 1.0 + \phi_n \leq 1.05 \quad \forall n \in N \quad (\text{M5.2})$$

$$q_n^c \leq M c_n \quad (\text{M5.3})$$

$$q_n \leq \bar{q}_n^g \quad \forall n \in G \quad (\text{M5.4})$$

$$q_n = \sum_{m \in N}^{n \neq m} \hat{q}_{nm}^t + \hat{q}_{nm}^\Delta \quad \forall n \in G \quad (\text{M5.5})$$

$$q_n - q_n^c = \sum_{m \in N}^{n \neq m} \hat{q}_{nm}^t + \hat{q}_{nm}^\Delta \quad \forall n \in N : n \neq s \wedge n \notin G \quad (\text{M5.6})$$

Constraints from Model 3 (The Cold-Start LPAC Model) except (M3.5)

TABLE X

CAPACITOR PLACEMENT: EFFECTS OF $|\underline{\tilde{V}}|$ ON IEEE57-C, $\bar{q}^c = 30$ MVAR

$ \underline{\tilde{V}} $	$\min(\underline{\tilde{V}})$	$\max(\underline{\tilde{V}})$	$\max(q_n)$	$\sum c_n$	Time (sec.)
0.8850	0.000000	0.0	0.0	1	1
0.9350	0.000000	0.0	0.0	3	8
0.9600	0.000000	0.0	0.0	5	156
0.9750	0.000000	0.0	0.0	6	177
0.9775	0.000000	0.0	0.0	6	139
0.9800	0.000000	0.0	0.0	6	75
0.9840	-0.000802	0.0	0.0	7	340

extremely accurate and only has minor constraint violations on the lower bounds of the voltage values. It is important to note that, although the CPP model can take as long as five minutes to prove optimality³, it often finds the best solution value within a few seconds. The voltage lower bound approaches the value of 0.985, which is the lowest value of the voltage-controlled generators in the benchmark. These results remain consistent for other voltage bounds.

Once again, the CPP model indicates the benefits of the LPAC approximation for decision-support applications that need to reason about reactive power and voltages.

VI. RELATED WORK

Many linearizations of the AC power flow equations have been developed [4], [6], [7], [16], [35], [39], [59]. Broadly, they can be grouped into iterative methods [6], [16], [59] and convex models [4], [7], [35], [39].

Iterative Methods: Iterative methods, such as the fast-decoupled load flow [59], significantly reduce the computation time of solving the AC equations and demonstrate sufficient accuracy. Their disadvantage however is that they cannot be efficiently integrated into traditional decision-support tools. Indeed, MIP solvers require purely declarative models to obtain lower bounds that are critical in reducing the size of the search space. Note however that, modulo the linear

³It is of course only optimal up the quality of the LPAC approximation.

approximations, the LPAC model can be viewed as solving a decoupled load flow globally. The key differences are:

- 1) Because the model forms one large linear system, all of the steps of the decoupled load flow are effectively solved simultaneously;
- 2) Because the formulation is a linear program, the values of p and q can now be decision variables, and bounds may be placed on the line capacities, voltage magnitudes, and phase angles;
- 3) The model may be embedded in a MIP solver for making discrete decisions about the power system.

The second and third points represent significant advantages over the fast-decoupled load flow and other iterative methods.

Convex Models: Although many variants of the LDC model exist, few declarative models incorporate reactive flows in cold-start contexts. To our knowledge, three cold-start approaches have been proposed: (1) a polynomial approximation scheme [39], (2) a semi-definite programming relaxation [7], and (3) a voltage-difference model [35].

The polynomial approximation has the advantage of solving a convex relaxation of the AC power equations but the number of variables and constraints needed to model the relaxation "grows rapidly" [39] and only second-order terms were considered. The accuracy of this approach for general power flows remains an open question: Reference [39] focuses on a transmission planning application and does not quantify the accuracy of the approximation relative to an AC power flow.

The semi-definite programming (SDP) relaxation [7] has the great advantage that it can solve the power flow equations precisely, without any approximation. In fact, reference [7] demonstrated that the formulation finds the globally optimal value to the AC optimal power flow problem on a number of traditional benchmarks. However, recent work has shown this does not hold on some practical examples [60]. Computationally, SDP solvers are also less mature than LP solvers and their scalability remains an open question [61]. Solvers integrating discrete variables on top of SDP models [62] are very recent and do not have the scientific maturity of MIP solvers [48].

The voltage-difference model [35] has a resemblance to a model combining the equation

$$\hat{p}_{nm}^h = |\tilde{V}_n^h|^2 g_{nm} - |\tilde{V}_n^h| |\tilde{V}_m^h| g_{nm} - |\tilde{V}_n^h| |\tilde{V}_m^h| b_{nm} (\theta_n^\circ - \theta_m^\circ)$$

with Equation (17). However, it makes a fundamental assumption that all voltages are the same before computing the voltage differences. In practice, voltage-controlled generators violate this assumption. On traditional power system benchmarks, we observed that the voltage-difference formulation had similar accuracy to the LDC model.

VII. CONCLUSION

This paper presented linear programs to approximate the AC power flow equations. These linear programs, called the LPAC models, capture both the voltage phase angles and magnitudes, which are coupled through equations for active and reactive power. The models use a piecewise linear approximation of the cosine term in the power flow equations. The cold-start

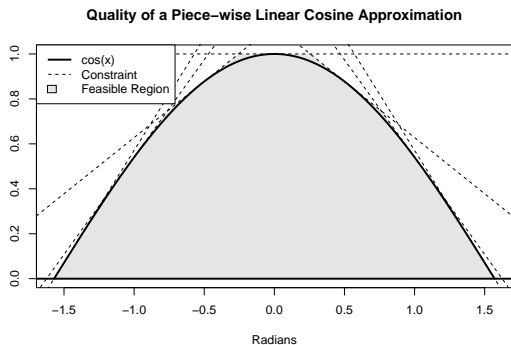


Fig. 4. A Piecewise-Linear Approximation of Cosine using 7 Inequalities.

and warm-start models use a Taylor series for approximating the remaining nonlinear terms.

The LPAC models have been evaluated experimentally over a number of standard benchmarks under normal operating conditions and under contingencies of various sizes. Experimental comparisons with AC solutions on a variety of standard IEEE and MatPower benchmarks shows that the LPAC models are highly accurate for active and reactive power, phase angles, and voltage magnitudes. The paper also presented two case studies in power restoration and capacitor placement to provide evidence that the cold-start and warm-start LPAC models can be efficiently used as a building block for optimization problems involving constraints on reactive power flow and voltage magnitudes. As a result, the LPAC models have the potential to broaden the success of the traditional LDC model into new application areas and to bring increased accuracy and reliability to current LDC applications.

There are many opportunities for further study, including the application of the LPAC models to a number of application areas. From an analysis standpoint, it would be interesting to compare the LPAC models with an AC solver using a “distributed slack bus”. Such an AC solver models the real power systems more accurately and provides a better basis for comparison, since the LPAC models are easily extended to flexible load and generation at all buses.

APPENDIX A

A LINEAR PROGRAMMING APPROXIMATION OF COSINE

The convex approximation of the cosine function is implemented through a piecewise linear function that produces a linear program in the following way. The modeler selects a desired domain $(l, h)^4$ and a number segments s . Then s tangent inequalities are placed on the cosine function within the provided domain to approximate the convex region. Figure 4 illustrates the approximation approach using seven linear inequalities. The dark black line shows the cosine function, the dashed lines are the linear inequality constraints, and the shaded area is the feasible region of the linear system formed by those constraints. The inequalities are obtained from tangents lines at various points on the function. Specifically,

⁴The domain should not exceed the range $(-\pi/2, \pi/2)$ to ensure convexity. In practice, $\theta_n^\circ - \theta_m^\circ$ is typically very small and a narrower domain is preferable.

```

PWL<COS>(xcos, x, l, h, s)
1  post(xcos ≥  $\frac{\cos(h) - \cos(l)}{h-l}(x-l) + \cos(l)$ )
2  inc ← (h - l)/(s + 1)
3  a ← l + inc
4  for i ∈ 1..s
5  do fa ← cos(a)
6     sa ← -sin(a)
7     post(xcos ≤ sax - saa + fa)
8     a ← a + inc

```

Fig. 5. Generating Evenly Spaced Piecewise-Linear Approximations.

for an x-coordinate a , the tangent line is $y = -\sin(a)(x-a) + \cos(a)$ and, within the domain of $(-\pi/2, \pi/2)$, the inequality

$$y \leq -\sin(a)(x - a) + \cos(a) \quad \forall a$$

holds. Figure 5 gives an algorithm to generate s inequalities evenly spaced within (l, h) . In the algorithm, x is a decision variable used as an argument of the cosine function and $x_{\widehat{\cos}}$ is a decision variable capturing the approximate value of $\cos(x)$.

REFERENCES

- [1] J. A. Momoh, *Electric Power System Applications of Optimization (Power Engineering (Willis))*. CRC Press, 2001.
- [2] A. Ott, “Unit commitment in the pjm day-ahead and real-time markets,” <http://www.ferc.gov/eventcalendar/Files/20100601131610-Ott,2010>, accessed: 22/04/2012.
- [3] J. Miller, “Power system optimization smart grid, demand dispatch, and microgrids,” Published online at <http://www.netl.doe.gov/smartgrid/referenceshell/presentations/SESept.2011>, accessed: 22/04/2012.
- [4] Z. Wang, D. Peng, Q. Feng, H. Liu, and D. C. Yu, “A non-incremental model for optimal control of reactive power flow,” *Electric Power Systems Research*, vol. 39, no. 2, pp. 153 – 159, 1996.
- [5] P. K. C. Aniruddha Bhattacharya, “Solution of optimal reactive power flow using biogeography-based optimization,” *International Journal of Electronics and Electrical Engineering*, vol. 4, no. 8, pp. 568 – 576, 2010.
- [6] D. Thukaram, K. Parthasarathy, and D. Prior, “Improved algorithm for optimum reactive power allocation,” *International Journal of Electrical Power and Energy Systems*, vol. 6, no. 2, pp. 72 – 74, 1984.
- [7] J. Lavaei and S. Low, “Zero duality gap in optimal power flow problem,” *IEEE Transactions on Power Systems*, vol. 27, no. 1, pp. 92 –107, feb. 2012.
- [8] S. Granville, “Optimal reactive dispatch through interior point methods,” *IEEE Transactions on Power Systems*, vol. 9, no. 1, pp. 136 –146, feb 1994.
- [9] P. Sreejaya and S. Iyer, “Optimal reactive power flow control for voltage profile improvement in ac-dc power systems,” in *Joint International Conference on Power Electronics, Drives and Energy Systems (PEDES) 2010 India*, dec. 2010, pp. 1 –6.
- [10] N. Deeb and S. Shahidehpour, “Linear reactive power optimization in a large power network using the decomposition approach,” *IEEE Transactions on Power Systems*, vol. 5, no. 2, pp. 428 –438, may 1990.
- [11] V. Ajarapu, P. L. Lau, and S. Battula, “An optimal reactive power planning strategy against voltage collapse,” *IEEE Transactions on Power Systems*, vol. 9, no. 2, pp. 906 –917, may 1994.
- [12] D. Kirschen and H. Van Meerteren, “Mw/voltage control in a linear programming based optimal power flow,” *IEEE Transactions on Power Systems*, vol. 3, no. 2, pp. 481 –489, may 1988.
- [13] J. Momoh, R. Adapa, and M. El-Hawary, “A review of selected optimal power flow literature to 1993. i. nonlinear and quadratic programming approaches,” *IEEE Transactions on Power Systems*, vol. 14, no. 1, pp. 96 –104, feb 1999.
- [14] J. Momoh, M. El-Hawary, and R. Adapa, “A review of selected optimal power flow literature to 1993. ii. newton, linear programming and interior point methods,” *IEEE Transactions on Power Systems*, vol. 14, no. 1, pp. 105 –111, feb 1999.
- [15] T. Overbye, X. Cheng, and Y. Sun, “A comparison of the ac and dc power flow models for Imp calculations,” in *Proceedings of the 37th Annual Hawaii International Conference on System Sciences*, 2004.

- [16] A. R. S.G. Seifossadat, M. Saniei, "Reactive power pricing in competitive electric markets using a sequential linear programming with considered investment cost of capacitor banks," *The International Journal of Innovations in Energy Systems and Power*, vol. 1, April 2009.
- [17] J. R. A. Munoz, "Analysis and application of optimization techniques to power system security and electricity markets," Ph.D. dissertation, University of Waterloo, 2008.
- [18] E. Fisher, R. O'Neill, and M. Ferris, "Optimal transmission switching," *IEEE Transactions on Power Systems*, vol. 23, no. 3, pp. 1346–1355, 2008.
- [19] K. Hedman, R. O'Neill, E. Fisher, and S. Oren, "Optimal transmission switching with contingency analysis," *IEEE Transactions on Power Systems*, vol. 24, no. 3, pp. 1577–1586, aug. 2009.
- [20] A. Khodaei and M. Shahidehpour, "Transmission switching in security-constrained unit commitment," *IEEE Transactions on Power Systems*, vol. 25, no. 4, pp. 1937–1945, nov. 2010.
- [21] B. Wollenberg and W. Stadlin, "A real time optimizer for security dispatch," *IEEE Transactions on Power Apparatus and Systems*, vol. PAS-93, no. 5, pp. 1640–1649, sept. 1974.
- [22] B. Stott, J. Marinho, and O. Alsac, "Review of linear programming applied to power system rescheduling," in *Power Industry Computer Applications Conference, 1979 (PICA-79)*, may 1979, pp. 142 – 154.
- [23] F. Lee, J. Huang, and R. Adapa, "Multi-area unit commitment via sequential method and a dc power flow network model," *IEEE Transactions on Power Systems*, vol. 9, no. 1, pp. 279–287, feb 1994.
- [24] M. Shahidehpour, H. Yamin, and Z. Li, *Market Operations in Electric Power Systems: Forecasting, Scheduling, and Risk Management*. Wiley-IEEE Press, 2002.
- [25] H. Pinto, F. Magnago, S. Brignone, O. Alsac, and B. Stott, "Security constrained unit commitment: Network modeling and solution issues," in *Power Systems Conference and Exposition, 2006. PSCE '06. 2006 IEEE PES*, 29 2006–nov. 1 2006, pp. 1759–1766.
- [26] C. A. N. A Borghetti, M Paolone, "A Mixed Integer Linear Programming Approach to the Optimal Configuration of Electrical Distribution Networks with Embedded Generators," *Proceedings of the 17th Power Systems Computation Conference (PSCC'11), Stockholm, Sweden*, 2011.
- [27] E. Romero-Ramos, J. Riquelme-Santos, and J. Reyes, "A simpler and exact mathematical model for the computation of the minimal power losses tree," *Electric Power Systems Research*, vol. 80, no. 5, pp. 562 – 571, 2010.
- [28] P. C. Roberto S. Aguiar, "Capacitor placement in radial distribution networks through a linear deterministic optimization model," *Proceedings of the 15th Power Systems Computation Conference (PSCC'05), Lige, Belgium*, 2005.
- [29] M. Delfanti, G. Granelli, P. Marannino, and M. Montagna, "Optimal capacitor placement using deterministic and genetic algorithms," *IEEE Transactions on Power Systems*, vol. 15, no. 3, pp. 1041–1046, aug 2000.
- [30] Y.-C. Huang, H.-T. Yang, and C.-L. Huang, "Solving the capacitor placement problem in a radial distribution system using tabu search approach," *IEEE Transactions on Power Systems*, vol. 11, no. 4, pp. 1868–1873, nov 1996.
- [31] D. Bienstock and S. Mattia, "Using mixed-integer programming to solve power grid blackout problems," *Discrete Optimization*, vol. 4, no. 1, pp. 115– 141, 2007.
- [32] M. K. Mangoli, K. Y. Lee, and Y. M. Park, "Optimal long-term reactive power planning using decomposition techniques," *Electric Power Systems Research*, vol. 26, no. 1, pp. 41 – 52, 1993.
- [33] A. Hughes, G. Jee, P. Hsiang, R. Shoults, and M. Chen, "Optimal reactive power planning," *IEEE Transactions on Power Apparatus and Systems*, vol. PAS-100, no. 5, pp. 2189–2196, may 1981.
- [34] K. Lee and F. Yang, "Optimal reactive power planning using evolutionary algorithms: a comparative study for evolutionary programming, evolutionary strategy, genetic algorithm, and linear programming," *IEEE Transactions on Power Systems*, vol. 13, no. 1, pp. 101–108, feb 1998.
- [35] A. M. C. A. Koster and S. Lemkens, "Designing ac power grids using integer linear programming," in *INOC*, ser. Lecture Notes in Computer Science, J. Pahl, T. Reinert, and S. Voß, Eds., vol. 6701. Springer, 2011, pp. 478–483.
- [36] R. Jabr, "Optimal placement of capacitors in a radial network using conic and mixed integer linear programming," *Electric Power Systems Research*, vol. 78, no. 6, pp. 941 – 948, 2008.
- [37] X. Wang and J. McDonald, *Modern Power System Planning*. McGraw-Hill (Tx), 1994.
- [38] J. dos Santos, A., P. Franca, and A. Said, "An optimization model for long-range transmission expansion planning," *IEEE Transactions on Power Systems*, vol. 4, no. 1, pp. 94 –101, feb 1989.
- [39] J. Taylor and F. Hover, "Linear relaxations for transmission system planning," *IEEE Transactions on Power Systems*, vol. 26, no. 4, pp. 2533–2538, nov. 2011.
- [40] J. Salmeron, K. Wood, and R. Baldick, "Analysis of electric grid security under terrorist threat," *IEEE Transactions on Power Systems*, vol. 19, no. 2, pp. 905– 912, 2004.
- [41] —, "Worst-case interdiction analysis of large-scale electric power grids," *IEEE Transactions on Power Systems*, vol. 24, no. 1, pp. 96–104, 2009.
- [42] N. Peterson, W. Tinney, and D. Bree, "Iterative linear ac power flow solution for fast approximate outage studies," *IEEE Transactions on Power Apparatus and Systems*, vol. PAS-91, no. 5, pp. 2048–2056, sept. 1972.
- [43] P. Ruiz and P. Sauer, "Post-contingency voltage and reactive power estimation and large error detection," in *Power Symposium, 2007. NAPS '07. 39th North American*, 30 2007–oct. 2 2007, pp. 266–272.
- [44] D. Bienstock and A. Verma, "The n-k problem in power grids: New models, formulations, and numerical experiments," *SIAM Journal on Optimization*, vol. 20, no. 5, pp. 2352–2380, 2010.
- [45] C. Coffrin, P. Van Hentenryck, and R. Bent, "Strategic stockpiling of power system supplies for disaster recovery," *Proceedings of the 2011 IEEE Power & Energy Society General Meetings (PES)*, 2011.
- [46] P. Van Hentenryck, C. Coffrin, and R. Bent, "Vehicle routing for the last mile of power system restoration," *Proceedings of the 17th Power Systems Computation Conference (PSCC'11), Stockholm, Sweden*, 2011.
- [47] B. Stott, J. Jardim, and O. Alsac, "Dc power flow revisited," *IEEE Transactions on Power Systems*, vol. 24, no. 3, pp. 1290–1300, 2009.
- [48] R. Bixby, M. Fenelon, Z. Gu, E. Rothberg, and R. Wunderling, *System Modelling and Optimization: Methods, Theory, and Applications*. Kluwer Academic Publishers, 2000, ch. MIP: Theory and practice – closing the gap, pp. 19–49.
- [49] K. Purchala, L. Meeus, D. Van Dommelen, and R. Belmans, "Usefulness of DC power flow for active power flow analysis," *Power Engineering Society General Meeting*, pp. 454–459, 2005.
- [50] C. Coffrin, P. Van Hentenryck, and R. Bent, "Approximating Line Losses and Apparent Power in AC Power Flow Linearizations," *Proceedings of the 2012 IEEE Power & Energy Society General Meetings (PES)*, 2012.
- [51] —, "Smart Load and Generation Scheduling for Power System Restoration," *Proceedings of the 2012 IEEE Power & Energy Society General Meetings (PES)*, 2012.
- [52] U. G. Knight, *Power systems engineering and mathematics*, by U. G. Knight. Pergamon Press Oxford, New York., 1972.
- [53] A. J. Wood and B. F. Wollenberg, *Power Generation, Operation, and Control*. Wiley-Interscience, 1996.
- [54] L. Powell, *Power System Load Flow Analysis (Professional Engineering)*. McGraw-Hill Professional, 2004.
- [55] A. Gomez-Exposito, A. J. Conejo, and C. Canizares, *Electric Energy Systems: Analysis and Operation (Electric Power Engineering Series)*. CRC Press, 2008.
- [56] J. Grainger and W. S. Jr., *Power System Analysis*. McGraw-Hill Science/Engineering/Math, 1994.
- [57] U. of Washington Electrical Engineering, "Power systems test case archive," <http://www.ee.washington.edu/research/pstca/>, accessed: 30/04/2012.
- [58] R. Zimmerman, C. Murillo-S andnchez, and R. Thomas, "Matpower: Steady-state operations, planning, and analysis tools for power systems research and education," *IEEE Transactions on Power Systems*, vol. 26, no. 1, pp. 12–19, feb. 2011.
- [59] B. Stott and O. Alsac, "Fast decoupled load flow," *IEEE Transactions on Power Apparatus and Systems*, vol. 93, no. 3, pp. 859–869, 1974.
- [60] B. Lesieutre, D. Molzahn, A. Borden, and C. DeMarco, "Examining the limits of the application of semidefinite programming to power flow problems," in *49th Annual Allerton Conference on Communication, Control, and Computing (Allerton), 2011*, sept. 2011, pp. 1492–1499.
- [61] H. Mittelmann, "Benchmarks for optimization software," <http://plato.asu.edu/bench.html>, April 2012, accessed: 22/04/2012.
- [62] J. Lofberg, "Yalmip : a toolbox for modeling and optimization in matlab," in *2004 IEEE International Symposium on Computer Aided Control Systems Design*, sept. 2004, pp. 284–289.